

Test of cosmic isotropy in the Planck era

Yabebal T. Fantaye

Departement of Mathematics, University of Tor Vergata Roma2, Rome, Italy Email: fantaye@mat.uniroma2.it

Part of the talk is presented on behalf of the Planck Collaboration.

The two fundamental assumptions in cosmology are that the Universe is statistically homogeneous and isotropic when averaged on large scales. Given the big implication of these assumptions, there has been a lot of statistical tests carried out to verify their validity. Since the first high-precision Cosmic Microwave Background (CMB) data release by the WMAP satellite, many anomalies that challenges the isotropy assumption, including dipolar power asymmetry on large angular scales, have been reported. In this talk I will present a brief summary of the test of cosmic isotropy we carried out in the latest WMAP and Planck temperature data.

1 Introduction

The European Space Agency (ESA) Planck satellite mission has recently produced the most accurate picture of the Universe by measuring the CMB with unprecedented precision. The scientific findings of this mission is presented in a series of science papers, which are mostly consistent with that of WMAP, the previous CMB satellite experiment by NASA. These papers^a present a simple but challenging picture of the Universe. Despite being consistent with the standard picture, the Universe seen by Planck has some anomalies whose interpretation might require a new physics.

Amongst the Planck confirmed CMB anomalies the hemispherical power asymmetry^{1,2} is one of the major one. This anomaly implies that the distribution of power in one side of the universe is different from that of the opposite one, leading to a breakdown of cosmic isotropy. In general, it is assumed that on large scales, scales that are not processed by non-linear gravity, the Universe is homogeneous and isotropic. The former implies that if we are able to zoom out and look at larger patches of the Universe, the statistical property of these patches should be the same; while the latter means if we set ourselves at one point, like on earth, and see all around us the statistical property of the universe in one direction should be similar to another one, hence rotation invariant.

The significance of the hemispherical power asymmetry, however, has often been called into question, in particular, due to the alleged *a-posteriori* nature of the statistics used; the significance of the anomaly is calculated using a statistical method that is designed to detect the observed feature. The challenge to this criticism was first given by³ who showed that the 5-year WMAP data show a similar trend up to $\ell = 600$. Moreover, using an alternative approach which modelled the power asymmetry in terms of a dipolar modulation field, as suggested by^{4,5} found a 3.3σ detection using data smoothed to an angular resolution of 4.5° FWHM, with an axis in excellent agreement with previous results.

^a<http://sci.esa.int/planck/51551-simple-but-challenging-the-universe-according-to-planck/>.

In this talk I will present a brief summary of the test of cosmic isotropy we carried out in the latest WMAP and Planck temperature data.

2 Power asymmetry analysis methods

There are in general two methods employed to test power asymmetry in the CMB map. The first one is to compute local-power on a disc at different sky directions and compare their consistency with isotropic power distribution. The effect of mask, noise and other complications are incorporated in such a method by using a set of simulations which are processed in a similar way to the data. The excess mismatch between the distribution of local-power in the data and simulations serve as a measure of significance of the power asymmetry. The second one is to assume a dipolar or higher order power asymmetry model and do a likelihood analysis. The two common analyses in this category are the pure dipole modulation by ⁵ and the generalised dipole modulation model as implemented in Bipolar spherical harmonics (BiPoSHs) technique ⁶.

In our analyses of the WMAP and Planck data in ^{7,9}, we quantified the degree of anisotropy by measuring the distribution of local-power, which is measured as the variance or power spectrum of the local patches, in the CMB maps. The variance of a map is related to its power spectrum as

$$\sigma^2 = \frac{1}{4\pi} \sum_{\ell=0}^{\ell_{max}} (2\ell + 1)C_{\ell}, \quad (1)$$

and hence using both of these quantities offers a possibility to study any deviation from isotropy in both real and harmonic space. Moreover, using power spectrum allows us easily study the scale dependence of a possible power variation in the CMB maps, while using variance we avoid mask induced complications in harmonic decomposition.

To incorporate a scale dependence study to the variance based method, we decomposed the map in to needlet components.

$$\beta_j(n) = \sum_{\ell=B^{j-1}}^{B^{j+1}} b^2\left(\frac{\ell}{B^j}\right)T_{\ell}(n), \quad (2)$$

where $T_{\ell}(n)$ denotes the component at multipole ℓ of the CMB map $T(n)$, e.g.

$$T(n) = \sum_{\ell} T_{\ell}(n),$$

$n \in S^2$ denotes the pointing direction, B is a fixed parameter (usually taken to be between 1 and 2) and $b(\cdot)$ is a smooth function such that $\sum_j b^2(\frac{\ell}{B^j}) = 1$ for all ℓ .

The advantage of using needlets is that the needlet filter has a very good localisation property both in pixel and harmonic space, and the needlet component maps are minimally affected by masked regions, especially at high-frequency. In particular, of course the multipole components $T_{\ell}(n)$ cannot be reconstructed on masked data; nevertheless their linear combination (2) can be shown to be very robust to the presence of gaps, and more so on small scales/high frequencies.

In what follows we will refer the local-power method with variance measure as *local-variance* and local-power with power spectra measures as *local- C_{ℓ}* . A summary of the procedures we followed in both of these methods are as follows:

1. create a binary patch mask which are centred on low resolution **HEALPix** ¹⁰ pixels. For both local- C_{ℓ} and local-variance methods we have considered 3072 ($N_{\text{inside}} = 16$) highly overlapping disc patches covering the entire sky. The radius of the discs varies from 1 to 90

degrees. The final local- C_ℓ results, however, are quoted from analysis performed using 12 non-overlapping patches, the base HEALPix $N_{\text{inside}} = 1$ pixels. We have shown that there is no significant difference between the results obtained using overlapping or non-overlapping patches.

2. looping over patch numbers, create an analysis patch mask by multiplying the binary disc mask with that of a foreground confidence and point source masks. In the case of local- C_ℓ analysis, we have apodised the foreground confidence and point source masks to reduce correlations between modes.
3. apply the analysis patch mask to the CMB + noise maps which are either the WMAP and Planck data or realistic simulations.
4. for each patch compute $C_{\ell s}$ using the MASTER technique¹¹ in bins of 16 multipoles; or variance of the unmasked pixels. For the local- C_ℓ case, the MASTER $16 - \ell$ blocks are further binned into $100 - \ell$ blocks to reduce bin to bin correlations as well as to compare our results with previous similar analyses.
5. for each patch estimate the mean and variance of local- C_ℓ or local-variance using N_{sim} realistic simulations. The mean is used to subtract the local mean-field from both data and simulations, while the variance is used to weight the corresponding patch.
6. estimate dipole amplitude and dipole directions of the local-power map using the HEALPix routine `remove_dipole` by applying an inverse variance weighting.

3 Results and Discussion

In this section I will present the summary of results presented in^{7,9}, and some updates which are not included in these published papers. In particular, I will describe the result we obtained using the local-variance analysis on needlet decomposed maps.

As outlined in the previous section, our test statistics is based on dipole amplitudes and dipole directions of the data and simulation local-power maps. For local- $C_{\ell s}$, which are estimated in $100 - \ell$ blocks, we obtained $\ell_{\text{max}}/100$ $N_{\text{inside}} = 1$ local- C_ℓ maps. For WMAP and Planck $\ell_{\text{max}} = 600$ and $\ell_{\text{max}} = 1500$ is used, which are corresponding to 6 and 15 dipole amplitude and directions, respectively. On the other hand, for the local-variance analysis we used 20 disc sizes with radius ranging from 1-90 degrees, and obtained 20 dipole amplitudes and directions. The later case is estimated for both the original real-space maps and the corresponding needlet decomposed maps.

In all cases we have used p-values to quantify the significance of the observed power asymmetry. The p-values are computed by comparing the anisotropic signal measured by our test-statistics, magnitude of dipole amplitudes or clustering of dipole directions, with those obtained from realistic simulations. For the WMAP case, we generated 1000 CMB-plus-noise Monte Carlo (MC) simulations based on the WMAP9 best-fit Λ CDM power spectrum¹². Noise realisations are drawn as uncorrelated Gaussian realisations with a spatially varying RMS distribution given by the number of observations per pixel. For Planck we adopt the 1000 ‘‘Full Focal Plane’’ (FFP6) end-to-end simulations produced by the Planck collaboration based on the instrument performance and noise properties. These simulations also incorporate lensing and component separation effects. The simulations are treated identically to the data in all steps discussed below.

Using dipole modulated simulations, we found that clustering of dipole directions is more sensitive to measuring a small power asymmetry signal, small dipole modulation amplitudes, than comparing the magnitude of dipole amplitudes in data and simulations. The dipole directions clustering, however, can only be obtained when there are at least a few number of

independent dipole direction estimates, which is only the case for local- C_ℓ analysis. For the local-variance method, however, the dipole directions for different disc sizes are correlated, and hence we can not use the alignment of dipole directions as a measure of significance. We compute p-values, therefore, based on excess of the data dipole amplitude from those of the simulations.

3.1 local- C_ℓ analysis

In⁷ we performed a local- C_ℓ analysis on WMAP 9-year data using 12 patches. We found that the power asymmetry is statistically significant at the 3.2σ confidence level for $\ell = 2-600$, where the data is signal dominated. The preferred asymmetry direction is $(l, b) = (227, -27)$, consistent with previous claims. Individual asymmetry axes estimated from six independent multipole ranges are all consistent with this direction.

In the same paper, we did also MCMC analysis on the 12 independent patches to determine the local best-fit values of the six Λ CDM cosmological parameters: the Hubble constant today (H_0); fractional densities of baryons (Ω_b), cold dark matter (Ω_m) and cosmic curvature (Ω_k); the reionization optical depth (τ); the amplitude (A_s) and spectral index (n_s) of the initial scalar fluctuations. Since most of the information used to constrain these parameters comes from the CMB power spectrum, the observed power asymmetry may have been caused by asymmetry in one or more of these cosmological parameters. After doing local-MCMC analysis, we obtained a map of local best-fit values for each six parameters. Since we used all multipole blocks of the MASTER power spectra for a given patch to estimate the parameters, we obtain only a single dipole amplitude and direction per parameter per map. As a result of this we can not use the dipole directions to measure significance of parameter asymmetry. The significance of parameter asymmetry is, therefore, measured by comparing the data and simulation local-best-fit map dipole amplitudes. We found that none of the cosmological parameters show a significant asymmetry. This is probably because of the large error bars in the parameters. It is, however, interesting to note that the dipole direction for the parameters A_s , n_s and Ω_b are in alignment with the power asymmetry direction, implying these parameters are the most sensitive to the power asymmetry observed.

The local- C_ℓ analysis of the Planck collaboration⁸ confirms a similar power asymmetry observed in the WMAP data, reassuring the power asymmetry is not due to systematic effects. This agreement across a wide range of scales as well as two different data sets clearly removes the statistical *a-posteriori* interpretation of the effect, and poses a new challenge for a detail investigation of the effect. In the Planck paper it was shown that the power asymmetry extends up to $\ell \sim 600$ with a significance of at least 3σ . Beyond this scale, however, the doppler boosting, which is due to the motion of our solar system barycenter with respect to the CMB, becomes dominant. Boosting is a significant contamination for power asymmetry study, and it has to be taken into account when looking for power asymmetry at small scales, large multipoles.

3.2 local-variance analysis

In⁹ we performed a local-variance analysis in both WMAP 9-year and Planck 1-year data. Left panel of Figure. (2) shows the results for Planck, which compares the dipole amplitudes of the data local-variance map (green stars) with that of the 1000 FFP6 simulations (grey stars) - none of the 1000 isotropic simulations have local-variance dipole amplitudes larger than the data over the range $6^\circ \leq r_{\text{disc}} \leq 12^\circ$. This implies that the variance in the Planck data exhibits a dipolar-like spatial variations that are statistically significant (at least) at the $\sim 3 - 3.5\sigma$ level or a p -value of less than 0.001. We showed that the distribution of the simulation dipole amplitudes are well fit by a Gaussian distribution for all discs sizes. The right panel of Figure. (2) visually illustrates mean-field subtracted local-variance map for the 6° radius disc. The dipole direction obtained from this map is $(l, b) = (212^\circ, -13^\circ)$.

Similar analysis using the WMAP 9-year data yields a statistical significance of $\sim 2.9\sigma$,

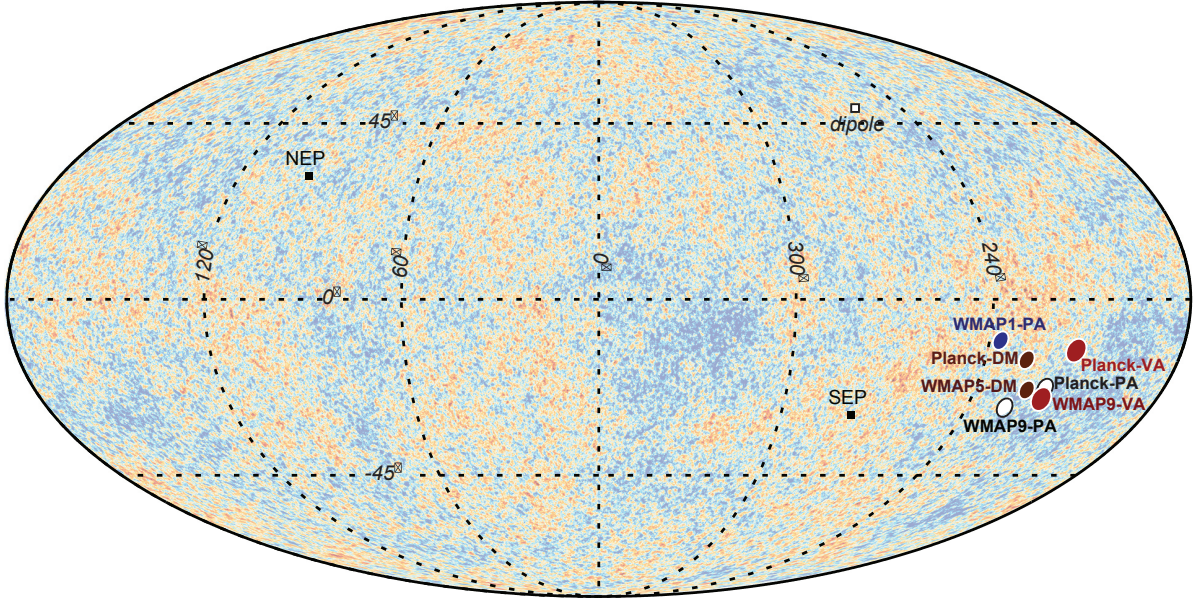


Figure 1 – Asymmetry directions found in different hemispherical power asymmetry analysis. The local variance of the WMAP 9-year and Planck 2013 data [denoted by WMAP9-VA and Planck-VA], as well as the directions found previously from the latest likelihood analyses of the dipole modulation model [denoted by WMAP5-DM and Planck-DM], and the local-power spectrum analyses [denoted by WMAP1-PA, WMAP9-PA and Planck-PA] for the WMAP and Planck data. The background map is the CMB sky observed by Planck (SMICA). VA, DM and PA stand for variance asymmetry, dipole modulation and power asymmetry, respectively. This figure is taken from Akrami et. al. 2013⁹.

and a direction fully consistent with those derived from Planck and other previous analyses. Our check shows that the difference in mask and input power spectra used to simulate the WMAP simulations seems to drive the difference in significance between Planck and WMAP, and a further investigation of this issue is necessary once the slight tension between WMAP and Planck data is resolved.

We have checked that the local-variance based results do not significantly change when we account for the doppler boosting effect either by including boosting in the simulations or by deboosting the data, similar to what we did for the Planck 143GHz channel map with the local- C_ℓ analysis. This is mostly because the local-variance method is mostly dominated by large scale modes where the effect of doppler boosting is small. As we will show below, however, this method actually is able to detect the boosting signal with $> 3\sigma$ significance when considering a high-pass filtered map.

The preferred directions obtained using local-variance and local- C_ℓ methods from our papers as well as a number of similar results obtained in previous papers are summarised in Figure 1.

3.3 Local-variance analysis on needlet components

To study the scale dependence of power asymmetry using the local-variance method, we decomposed the Planck SMICA data and FFP6 simulations into needlet components using (2), and performed the above analysis on each of the decomposed maps. The needlet parameters we used are such that a given map is decomposed into nine needlet component maps each having a compact support over a multipole range defined by $\ell = [B^{j-1}, B^{j+1}]$ where $j = 2, 3, \dots, 10$ and $B = 2$.

As shown in Figure. (3), all but the $j = 9$ needlet component have dipole amplitudes consistent with the FFP6 simulations - hence no significant power asymmetry. The $j = 9$ needlet map, which has a support to multipole ranges $\ell = [256, 1024]$, shows a significant anisotropy with p-value of 0.003, and with a dipole direction close to the CMB dipole. This means what we

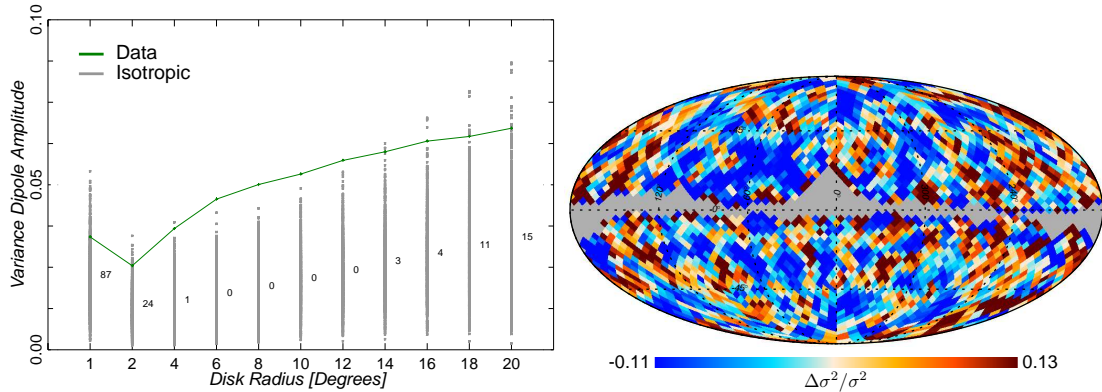


Figure 2 – Left panel: local-variance dipole amplitude as a function of disc radius for Planck SMICA data (in green) versus the 1000 isotropic FFP6 simulations (in grey). The labels above each scale indicate the number of simulations with amplitudes larger than the ones estimated from the data, and are located at the means of the amplitude values from the simulations. Right panel: mean-field subtracted, local-variance map computed with 6° discs for Planck data. This figure is taken from Akrami et. al. 2013⁹.

have detected in this component is not the power asymmetry we talked about in the previous paragraphs, but the well-know doppler boosting effect caused by our motion with respect to the CMB frame. This effect has been detected for the first time by Planck using a completely different algorithm¹³, and is used to measure our solar system barycenter velocity independent of the CMB dipole component. In addition, as shown in Figure. (4), the dipole direction of the $j = 10$ component has a dipole direction right on the CMB dipole. The Planck data local-variance dipole amplitude for this particular needlet component, however, is compatible with the FFP6 simulations. The reason for this may be due to the fact that the majority of the multipoles covered by the $j = 10$ component are sensitive to the boosting signal but with a small signal to noise values, while all of multipoles in the $j = 9$ component are signal dominated but with less sensitivity to the boosting signal, or possibly contaminated by a non-vanishing power asymmetry signal.

Some interesting features to note from Figure. (3) & (4) are: the dipole directions for the needlet component $j = 2 - 8$ are close to the power asymmetry direction; the dispersion of dipole amplitudes for isotropic simulations are large for small radius discs and becomes small for large discs. This is opposite to what we saw when using the full map. Of course, this is understandable since most of the needlet maps are not affected by the cosmic variance of the large scale modes.

The implication of Doppler boosting detection by our method implies that at least our method is sensitive to dipolar power asymmetry with amplitudes up to 0.1%. It is also a strong validation to our entire pipeline. Moreover, clustering of the lower multipole dipole directions, needlet components $j = 2 - 8$, to the power asymmetry dipole direction may hint existence of asymmetry at intermediate multipoles. Of course, a lot of verification work has to be done in this regard.

4 Summary

In this talk I have discussed the unique nature of the CMB in testing the statistical property of the Universe. Thanks to the high precision experiments like Planck, the test of cosmological principles, the assumption of statistical isotropy and homogeneity, is now becoming a major field in the CMB and large scale data analysis.

The current CMB data hints a lopsided Universe, more large scale structures in one side of the Universe than the other. The significance of this anomaly, however, is low, $< 4\sigma$, so one can not rule out yet the effect being just a statistical fluke. Moreover, although the persistence

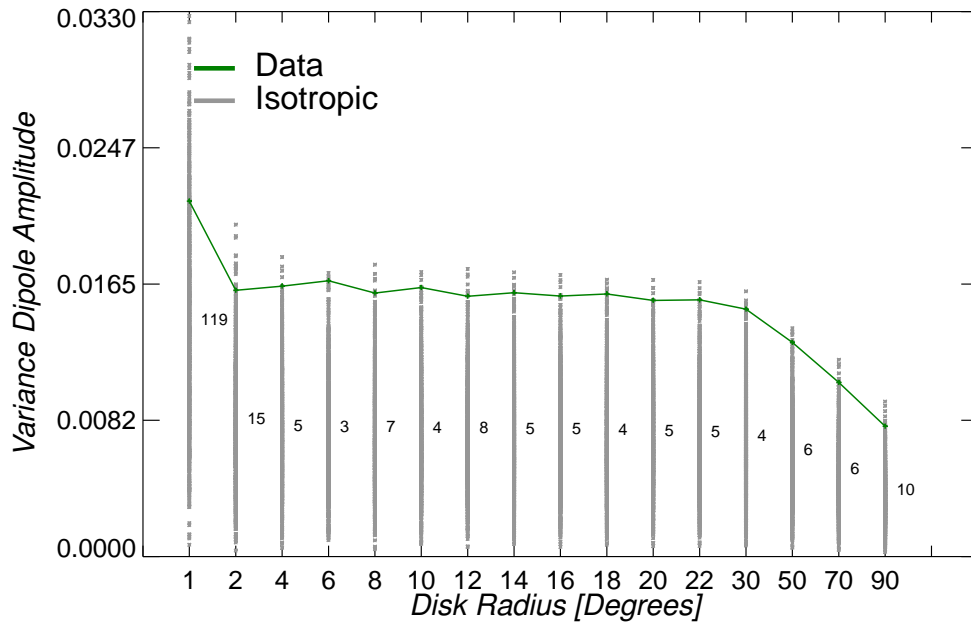


Figure 3 – Dipole amplitudes of the local-variance map for the $j = 9$, $256 \leq \ell \leq 1024$, needlet component as a function of disc radius. The Planck (SMICA) data (in green) versus the 1000 isotropic FFP6 simulations (in grey). The labels above each scale indicate the number of simulations with amplitudes larger than the ones estimated from the data.

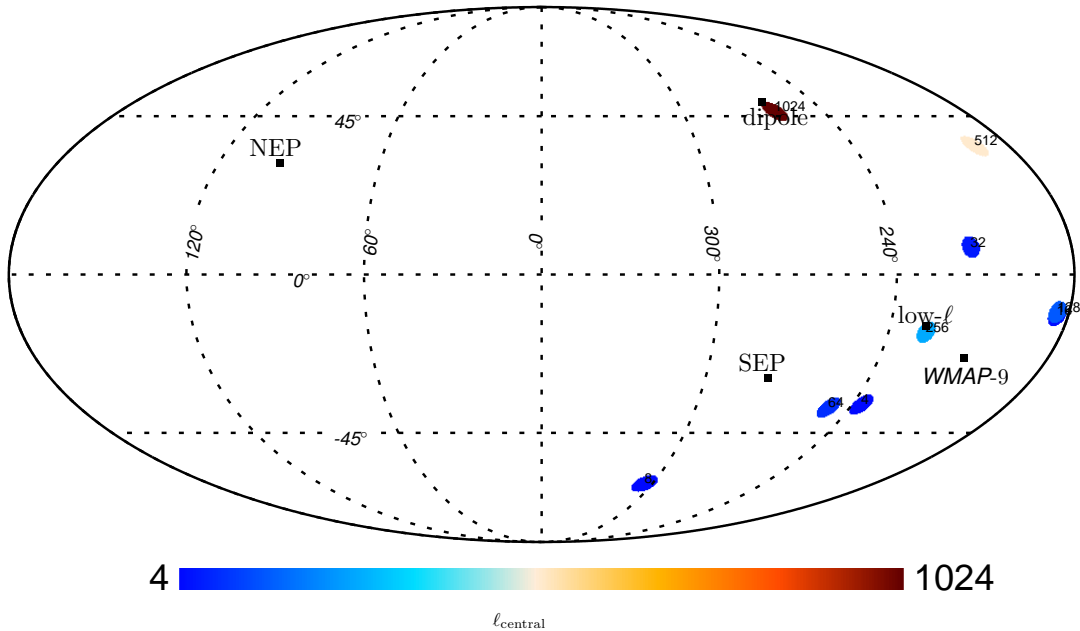


Figure 4 – Dipole directions of the local-variance maps of the nine needlet components, $j = 2, 3, \dots, 10$ with a disc radius of 90° . The labels in this plot indicates the central multipole of a given needlet map.

of the anomaly in both WMAP and Planck data seems to suggest the cause is unlikely to be foreground or systematic effects, we can not yet fully exclude the possibility of a local Universe phenomena. For this and other cases more work needs to be done to confirm the signal we are observing is truly cosmological. If that is proven, then this observation will represent another major discovery about the nature of our Universe and might lead to a new insight about the inner workings of inflation, which is responsible for laying out the initial conditions of the Universe from a mere quantum fluctuations.

In this endeavour there are different models in the literature trying to explain what is observed in the data, but to date there is no any single theoretical model that explains all the observations, power asymmetry both at large and intermediate scales.

While theorists are working out a viable model, there are going to be results from different experiments. For example, the full Planck temperature and polarisation data will be released in near future and it will be interesting to see what the outcomes will be. The planned CMB experiment PRISM¹⁴ promises to deliver a high-precision CMB polarisation maps. Since the statistical nature of polarisation maps as well as its systematics and foregrounds are not necessarily similar to that of the temperature maps, PRISM will be crucial in testing the isotropy hypothesis. On the other hand, EUCLID¹⁵, a space-based survey mission from ESA, will map the large scale structure with an unprecedented precision. Such observations will be able to test the isotropic assumption in the large scale structure, hence providing an independent verification. The future possibilities of the study and characterisation of the statistical nature of our Universe is therefore bright. These studies will ultimately contribute to our understanding of the processes that shaped the Universe from its birth to where it is now and where it is going.

Acknowledgments

This conference proceeding is a summary of the work I did in collaboration with M. Axelsson, Y. Akrami, A. Shafieloo, H. K. Eriksen, F. K. Hansen, A. J. Banday and K. M. Górski. This work is supported by ERC Grant 277742 Pascal. I acknowledge the use of resources from the Norwegian national super-computing facilities, NOTUR. Maps and results have been derived using the HEALPix (<http://healpix.jpl.nasa.gov>) software package developed by¹⁰.

References

1. H. K. Eriksen, F. K. Hansen, A. J. Banday, K. M. Gorski, and P. B. Lilje. Asymmetries in the Cosmic Microwave Background Anisotropy Field. *ApJ*, 605:14–20, April 2004.
2. F. K. Hansen, A. J. Banday, and K. M. Górski. Testing the cosmological principle of isotropy: local power-spectrum estimates of the WMAP data. *MNRAS*, 354:641–665, November 2004.
3. F. K. Hansen, A. J. Banday, K. M. Gorski, H. K. Eriksen, and P. B. Lilje. Power Asymmetry in Cosmic Microwave Background Fluctuations from Full Sky to Sub-degree Scales: Is the Universe Isotropic? *ApJ*, 704:1448–1458, 2009.
4. C. Gordon, W. Hu, D. Huterer, and T. Crawford. Spontaneous isotropy breaking: A mechanism for CMB multipole alignments. *Phys. Rev. D.*, 72(10):103002, November 2005.
5. J. Hoftuft, H. K. Eriksen, A. J. Banday, K. M. Gorski, F. K. Hansen, and P. B. Lilje. Increasing evidence for hemispherical power asymmetry in the five-year WMAP data. *ApJ*, 699:985–989, 2009.
6. A. Hajian and T. Souradeep. Testing global isotropy of three-year Wilkinson Microwave Anisotropy Probe (WMAP) data: Temperature analysis. *Phys. Rev. D.*, 74(12):123521, December 2006.
7. M. Axelsson, Y. Fantaye, F. K. Hansen, A. J. Banday, H. K. Eriksen, and K. M. Gorski. Directional dependence of Λ CDM cosmological parameters. *ArXiv e-prints*, March 2013.
8. Planck Collaboration, P. A. R. Ade, N. Aghanim, C. Armitage-Caplan, M. Arnaud, M. Ashdown, F. Atrio-Barandela, J. Aumont, C. Baccigalupi, A. J. Banday, and et al. Planck 2013 results. XXIII. Isotropy and Statistics of the CMB. *ArXiv e-prints*, March 2013.
9. Y. Akrami, Y. Fantaye, A. Shafieloo, H. K. Eriksen, F. K. Hansen, A. J. Banday, and K. M. Górski. Power asymmetry in WMAP and Planck temperature sky maps as measured by a local variance estimator. *ArXiv e-prints*, February 2014.
10. K. M. Górski, E. Hivon, A. J. Banday, B. D. Wandelt, F. K. Hansen, M. Reinecke, and M. Bartelmann. HEALPix: A Framework for High-Resolution Discretization and Fast Analysis of Data Distributed on the Sphere. *ApJ*, 699:759–771, April 2005.
11. E. Hivon, K. M. Górski, C. B. Netterfield, B. P. Crill, S. Prunet, and F. Hansen. MASTER of the Cosmic Microwave Background Anisotropy Power Spectrum: A Fast Method for Statistical Analysis of Large and Complex Cosmic Microwave Background Data Sets. *ApJ*, 567:2–17, March 2002.
12. G. Hinshaw et al. Nine-Year Wilkinson Microwave Anisotropy Probe (WMAP) Observations: Cosmological Parameter Results. *arXiv:1212.5226*, 2012.
13. Planck Collaboration, N. Aghanim, C. Armitage-Caplan, M. Arnaud, Ashdown, and et al. Planck 2013 results. XXVII. Doppler boosting of the CMB: Eppur si muove. *ArXiv e-prints*, March 2013.
14. PRISM Collaboration, P. Andre, C. Baccigalupi, D. Barbosa, and et. al. PRISM (Polarized Radiation Imaging and Spectroscopy Mission): A White Paper on the Ultimate Polarimetric Spectro-Imaging of the Microwave and Far-Infrared Sky. *ArXiv e-prints*, June 2013.
15. R. Laureijs, J. Amiaux, S. Arduini, J. . Auguères, J. Brinchmann, R. Cole, M. Cropper, C. Dabin, L. Duvet, A. Ealet, and et al. Euclid Definition Study Report. *ArXiv e-prints*, October 2011.